Modelling Space-time Periodic Structures with Arbitrary Unit Cells Using Time Periodic Circuit Theory

Sameh Y. Elnaggar, *Member, IEEE,* and Gregory N. Milford, *Senior Member, IEEE*

***Abstract*—Using the time periodic ABCD parameters, an expression for the dispersion relation of space-time modulated structures is obtained. The relation is valid for general structures even when the spatial granularity is comparable to the operating and modulation wavelengths. In the limit of infinitesimal unit cell, the dispersion relation reduces identically to its continuous counterpart. For homogeneous space-time modulated media, the time periodic circuit approach allows the extension of the well-known telegraphist's equations. The time harmonics are coupled together to form an infinite system of coupled differential equations. At the scattering centres, where the interaction is mediated via the modulation (pump wave), the telegraphist's equations reduce to the interaction of two waves only: the signal and idler. The interaction can then be described using three wave mixing, satisfying the phase matching condition. It is demonstrated that the time periodic S parameters provide an alternative and appealing visualization of the modal conversion and the emergence of non-reciprocity inside the bandgaps.**

***Index Terms*—Time Periodic, Space-time periodic, Nonreciprocity**

I. Introduction

The asymmetric interaction of space time harmonics in space-time modulated media has been recently exploited to design multitude of novel non-reciprocal devices such as magnet-less circulators [1]–[3], nonreciprocal antenna [4]–[6], one-way beam splitters [7], isolators via the exploitation of the asymmetric interband transition in a photonic crystal [8], [9], and manipulating wave transmission via a space time modulated metasurfaces [10], [11]. Additionally, it was demonstrated that the inclusion of time and/or space-time periodic elements can circumvent some physical limitations of linear time invariant systems. For instance, it was shown that an appropriately time modulated reactance can result in zero reflection and hence enables extreme energy accumulation [12]. Quite recently [13], it was theoretically shown that a system based on a time switched transmission line was demonstrated to have a broadband matching capability not limited by the Bode-Fano criteria [14]. Moreover, the modulation of both the effective permittivity and permeability was shown to enhance the nonreciprocity while still keeping the spacetime modulated structure perfectly matched to the host environment [15]. For a recent review on developments, applications and methods of analysis of space-time media, please refer to [16].

S.Y.E with the Electrical and Computer Engineering Department, Royal Military College of Canada, Kingston, Ontario. G.N.M are with the School of Engineering and Information Technology, University of New South Wales, Canberra, emails: samehelnaggar@gmail.com, g.milford@adfa.edu.au

Fundamentally, the modulation of a medium constitutive parameter by a travelling wave *biases* the transmission in one direction over the other(s), resulting in a skewed dispersion relation that cannot be achieved using space only or time only modulation [17], [18]. The theory of space-time modulated media dates back to the mid of last century when there was an immense interest in the study of distributed parametric interactions [19]–[24]. During that period, the theoretical foundation was established. The framework is based on Bloch-Floquet theory, where the variables (voltages and currents or electric and magnetic fields) are represented by an infinite sum of the space time harmonics. Upon the substitution of the variables into the governing differential equation (in this case the wave equation), the system behaviour can be expressed as the interaction of the infinite number of space time harmonics. Usually only few harmonics need to be considered, particularly in the vicinity of the scattering centres [18].

Practically speaking, lumped elements are used to synthesize space-time modulated structures; for instance, nonlinear elements (eg. varactors are periodically inserted in a host microstrip transmission line [25]). The modulation is introduced either using a strong pump wave on the same line or via a special arrangement where the modulation comes from another coupled transmission line [15], [25]. The operating regime is generally assumed and/or designed such that the granularity of the structure is small compared to the operating and modulation wavelengths; hence the structure is considered homogeneous.

Recently, it was shown that the scattering magnitude in a space-time modulated Right Handed Transmission Line (RH-TL) and subsequently the corresponding non-reciprocity can be enhanced by reducing the modulation wavelength λ_m [18]. For a given TL length, the reduction of the λ_m is equivalent to the increase of the interaction length. The analysis assumed the homogeneity of the underlying structure. Additionally as λ_m decreases so does the wavelength at the scattering centre. Eventually, the wavelengths are reduced to the extent that they may be just a few unit cells, raising the question about how short the modulation wavelength can be. Usually, the underlying medium was implicitly assumed to be RH, where either the shunt capacitor or series inductor is modulated.

The analogy between Linear Time Invariant (LTI) and Linear Time Periodic (LTP) circuits and systems has been exploited to analyze time periodic systems [26]–[28]. In RF circuits, time periodicity appears in oscillators and mixers, where a Periodic Transfer Function (PXF) is obtained after

the system is linearized around the steady state limit cycle [29]. Such analogy strongly suggests that an extension of the theory of periodic structures permits the exploration of arbitrary spacetime structures in a very similar fashion to that of space only periodic systems [30]. From the previous arguments, a framework that enables the characterization of arbitrary space-time periodic structures must be based on first principles: Floquet theorem and basic circuit theory. Being a circuit based approach, the *granularity* of the unit cells is automatically taken into account. It is required, of course, that the circuit based approach must reduce to the homogeneous case for an infinitesimally small unit cells. It is the aim of the current manuscript to develop such framework that generalizes the theory of periodic structures of LTI systems to enable the description of wave propagation in arbitrary space/time/spacetime periodic structures. For limiting cases (for instance as the modulation strength tends to zero or the structure becomes electrically small), the derived expressions reduce identically to their simpler counterparts.

It is worth noting that circuit based approaches have been successfully applied to describe and design time and space time periodic circuits. For instance, in [2], [3], [31] a circulator was built from three identical coupled resonators, where their resonant frequencies are temporally modulated and are 120° phase shifted from one another. The resonators were realized using lumped elements, where temporal modulation is introduced via varactors. In [4] a microstip line was capacitively loaded to permit coupling to free space. The capacitances were spatiotemporally modulated to break the symmetry between absorption and emission. The dispersion relation was calculated using a generalized circuit formalism based on the cascade of time periodic cells. Hence one of the purposes of the current article is to extend such an approach to arbitrary time, space and spacetime systems that are not necessarily electrically short. Such a treatement permits apparently different structures to be described by the same machinery and provides a unified framework capable of characterizing the physical interactions due to the complex coupling of space-time harmonics.

The first subsection in Section II briefly discusses the basics of time periodic circuits to highlight the analogy with LTI systems. Using the properties of time periodic circuits, the dispersion relation of an arbtirary spacetime periodic circuit is developed in subsection II-B. Additionally, under the long wavelength approximation, the space time periodic system is described by the extension of the well-known telegraphist's equations, representing space-time media by two coupled matrix equations. In Section III two examples are presented. The first example is a RH TL, where expressions of the dispersion relation and wave behaviour of modulated homogeneous media are well understood and thoroughly described in the literature. The wave interactions of a Composite Right Left Handed transmission line (CRLH TL) are explored as a second example to demonstrate the universality of the current approach.

II. Theory

A. Theoretical Background: Time Periodic Circuits

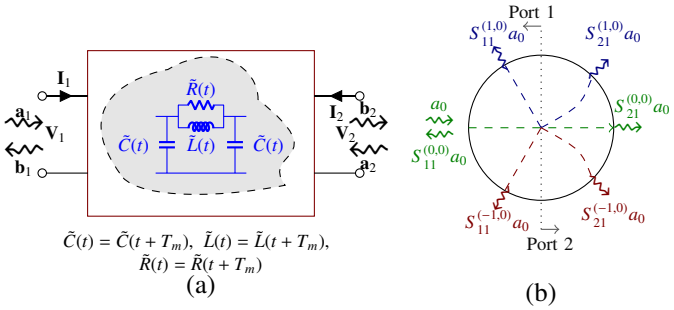

Fig. 1. (a) A generic time periodic circuit, consisting of an arbitrary number of time periodic inductors, capacitors and resistors. (b) Scattering from a generic time periodic circuit represented by the circle. The vertical dotted line conceptually separates between ports 1 and 2.

In this subsection, we briefly discuss time periodic circuits. It is worth noting that, although time periodic circuits have been investigated a long time ago [26], they have recently gained immense interest due to their intriguing properties such as their ability to anhilate reflections using reactive loads [12] and circumvent the Bode Fano bound [13]. Assume the arbitrary circuit shown in Fig. 1, where some of the circuit parameters (resistances, inductances or capacitances) are time periodic with a period T_m, where the subscript m stands for modulation. Although a time periodic two port network is shown in Fig. 1(a), the analysis is readily extendible to n ports networks. Given a general circuit as in Fig. 1(a), KVL and KCL can be applied to describe the circuit using a system of first order differential equations in the inductor currents and capacitor voltages, which define the system state vector $\mathbf{x}$ [32]. Generally speaking, the time evolution of $\mathbf{x}$ is represented by the well known state space matrix equation

$$\dot{\mathbf{x}} = \mathcal{A}(t)\mathbf{x} + \mathcal{B}(t)\mathbf{u}(t). \tag{1}$$

Due to the presence of time periodic elements in the circuit, $\mathcal{A}(t), \mathcal{B}(t)$ are real time periodic matrices determined from the circuit topology via KVL/KCL and $\mathbf{u}$ is the input vector excitation. Using Floquet theorem, for sinusoidal excitations with frequency ω, an arbitrary state x_l will attain the form [33], [34].

$$x_l(t) = p(t)e^{i\omega t} + c.c, \tag{2}$$

where $p(t) = p(t + T_m)$ is a periodic function and $c.c$ stands for the complex conjugate. Since $p(t)$ is periodic, (2) can be written as

$$x_l(t) = \sum_{k=-\infty}^{\infty} P_k e^{i\tilde{\omega}_k t} + c.c, \tag{3}$$

where P_k is the amplitude of the k^{th} harmonic of $p(t)$ and $\tilde{\omega}_k \equiv \omega + k\omega_m$. According to this notation, input frequency $\omega = \tilde{\omega}_0$, and hence ω and $\tilde{\omega}_0$ are synonymously used hereafter.

Substituting (3) back in (1) and noting that $\mathbf{x}$ represents currents and voltages, the coefficients of the p^{th} harmonic can be matched, resulting in a system of linear algebraic equations. The time periodic elements embedded in $\mathcal{A}$ and $\mathcal{B}$ couple the

p^{th} harmonic with other time harmonics. In the limiting case of linear time invariant (LTI) systems, the time harmonics are decoupled, allowing the state space variables to be determined at any given frequency ω, with no knowledge of the behaviour at other frequencies. For the general time periodic case, there is an infinite number of such equations (a set for each frequency $\tilde{\omega}_p$). Practically, only a few such harmonics are necessary to characterise performance. For instance if one is interested in the behaviour at the fundamental frequency $\tilde{\omega}_0$, the first finite time harmonics $2N+1$ ($|k| \leq N$) need only be considered, where N is usually small (1, 2 or3).

To elucidate the general approach, a simple circuit that consists of one shunt time periodic capacitance is analysed. Not only does it provide insight into the process, but also demonstrates how the concept of divide and conquer is applied, where complex systems can be divided into simpler cascaded subsystems. This concept is very useful in describing space-time periodic circuits, as will be shown in the next subsection. The current through the time periodic capacitance $\tilde{C}$ is given by

$$i(t) = \frac{d}{dt}\tilde{C}(t)v(t). \tag{4}$$

The periodicity of $\tilde{C}(t)$ allows its expansion in a Fourier series

$$\tilde{C}(t) = \sum_{k=-\infty}^{\infty} C_k e^{ik\omega_m t}. \tag{5}$$

Since $\tilde{C}(t)$ is real, $C_q = \bar{C}_{-q}$. Furthermore using (3), both $v(t)$ and $i(t)$ can be written as

$$v(t) = \sum_{r=-\infty}^{\infty} V_r e^{i\tilde{\omega}_r t} + c.c \text{ and } i(t) = \sum_{r=-\infty}^{\infty} I_r e^{i\tilde{\omega}_r t} + c.c \tag{6}$$

Substituting (5) and (6) in (4), and matching the $\exp(i\tilde{\omega}_r t)$ yield

$$I_p = \sum_{l=-\infty}^{\infty} i\tilde{\omega}_p C_{p-l} V_l = \sum_{l=-\infty}^{\infty} Y_{p-l} V_l, \tag{7}$$

where $Y_{p-l} \equiv i\tilde{\omega}_p C_{p-l}$ can be interpreted as the admittance connecting the l^{th} harmonic voltage with the p^{th} harmonic current. In another words, the p^{th} harmonic current is the sum of all currents due to *all* harmonic voltages. Defining the time periodic current and voltage as the infinite-dimensional vectors $\mathbf{I} = \left[\cdots, I_{p-1}, I_p, I_{p+1}, \cdots\right]^t$ and $\mathbf{V} = \left[\cdots, V_{p-1}, V_p, V_{p+1}, \cdots\right]^t$, (7) can be compactly written in a matrix form as

$$\mathbf{I} = \mathbf{Y}\mathbf{V} = i\Omega C\mathbf{V}, \tag{8}$$

where $\mathbf{Y}$ is the time periodic admittance, Ω is a diagonal matrix storing all harmonic frequencies $\tilde{\omega}_k$ and C is the time periodic capacitance matrix. Similar expressions for time periodic inductors and resistors can be obtained [26], [28]. As time harmonics go from $-\infty$ to ∞, where 0 labels the fundamental frequency, it is convenient to number the rows and columns of the matrices with reference to the fundamental component. According to this notation, the 0^{th} row denotes the fundamental component.

If a time periodic capacitance is connected in shunt between input and output terminals, the structure forms a two port network, where at $\tilde{\omega}_p$ the input voltage and current ($\mathbf{V}_1$ and $\mathbf{I}_1$) are related to the output values ($\mathbf{V}_2$ and $\mathbf{I}_2$) by the ABCD parameters,

$$\begin{bmatrix}\mathbf{V}_1\\ \mathbf{I}_1\end{bmatrix} = \begin{bmatrix}[\mathbf{A}] & [\mathbf{B}]\\ [\mathbf{C}] & [\mathbf{D}]\end{bmatrix}\begin{bmatrix}\mathbf{V}_2\\ \mathbf{I}_2\end{bmatrix}, \tag{9}$$

where $[\mathbf{A}]$, $[\mathbf{D}]$ are the identity matrices, $[\mathbf{B}]$ is the zero matrix and $[\mathbf{C}]$ (not to be confused with the capacitance matrix C) is the matrix where its (m,n) element is given by $C_{m,n} = Y_{m-n}$. The time periodic ABCD matrix is a generalization of the well-known ABCD matrix of LTI systems. In Ref. [26], *equivalent* voltages and currents were used to assure that the ABCD matric is frequency independent. Unlike Ref. [26], different type of elements can be included in the ABCD matrix. Depending on the circuit configuration, some circuit parameters can be more convenient than others. For instance, shunt (series) elements are naturally represented by the Y (Z) parameters. The conversion process between different sets of parameters parallels that of LTI systems [35].

Generally, each parameter is an infinite dimensional square matrix (hence the inner brackets), but practically only few harmonic need to be considered. In the subsequent analysis, for simpler notation, the inner brackets will be dropped. For a time periodic system, the conventional S-parameters (S_{11}, S_{21}, S_{12} and S_{22}) are extended to four matrices. The $\mathbf{S}_{11}$ represents the reflection coefficients at port number 1, when port 2 is terminated in the reference impedance. For instance, with reference to Fig. 1(b), consider an incident wave with frequency ω and complex amplitude a_0. $S_{11}^{(r,0)}a_0$ represents the wave bouncing back at port 1 in the r^{th} harmonic. Similarly, $S_{21}^{(r,0)}a_0$ is the wave transmitted to port 2 in the r^{th} harmonic.

B. Space-time Periodic Structures

The analysis in subsection II-A is general for time periodic systems. However sometimes, a system is also periodic in the spatial domain, forming a travelling wave modulation. This can result, for instance, from the linearization of nonlinear distributed structures [36] or the Distributedly Modulated Capacitance technique [25]. In this subsection, we will extend the time periodic circuit approach discussed in the previous section to space-time periodic structures.

Fig. 2 shows a hypothetical space-time periodic structure, where the modulation, regardless of it source, is represented by a travelling wave $G(t - x/v_m)$, where v_m is the wave front velocity. Accordingly, the wave front travels a unit cell length p in p/v_m units of time. The wave G can be the modulated capacitance, inductance or resistance. Generally, the spatially modulated elements are placed p units apart or at $x = np$, where n is an integer. There can be any number of modulated elements per unit cell, for instance a shunt capacitance or both capacitance and inductance of a right handed transmission line as in [15]. In this case there will be a travelling wave $G(t - x/v_m)$ for each modulated element and all travel with the same speed v_m. Any travelling wave G can then be written as

$$G(t - x/v_m) = G(t'), \tag{10}$$

where $t' = t - x/v_m$. $G(t')$ is periodic with a period T_m, therefore

$$G(t') = \sum_{r=-\infty}^{\infty} G^r \exp(ir[\omega_m t - \beta_m x]), \tag{11}$$

where $\beta_m \equiv \omega_m/v_m$ is the modulation wave number. In the long wavelength approximation, the exact positions of the modulated elements and the distance between them are irrelevant as long as p is much smaller than the operating and modulation wavelengths. We seek a general solution that satisfies the Bloch-Floquet condition (2) and (3), but in $t' = t - x/v_m$. Therefore, the harmonics components of v_{n+1} (i_{n+1}) and v_n (i_n) are related by

$$\mathbf{V}_{n+1} = \mathbf{P}_s \mathbf{V}_n, \tag{12}$$

where $\mathbf{P}_s$ is diagonal with $P_s^{rr} = \exp(-i\tilde{\beta}_r p)$ and $\tilde{\beta}_r \equiv \beta + r\beta_m$ is the wave number of the r^{th} harmonic. $\mathbf{P}_s$ can be thought of as the spatial (hence the s subscript) propagator; it relates the voltage and current at $x = (n+1)p$ to those at $x = np$.

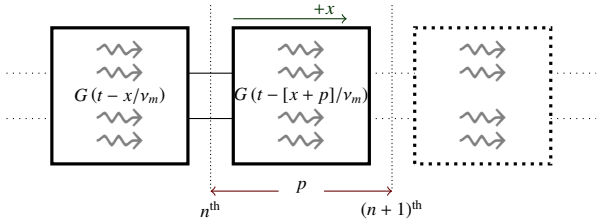

Fig. 2. An arbitrary space-time periodic structure with a unit cell of p units of length. The wiggly arrows emphasize the modulation in the spatial domain.

1) Generalized Dispersion Relation: Using (12) the dispersion relation can be determined from the solution of

$$F(\omega,\beta) \equiv \left\| \begin{bmatrix} \mathbf{A} & \mathbf{B} \\ \mathbf{C} & \mathbf{D} \end{bmatrix} \begin{bmatrix} \mathbf{P}_s & \mathbf{0} \\ \mathbf{0} & \mathbf{P}_s \end{bmatrix} - \begin{bmatrix} \mathbf{I} & \mathbf{0} \\ \mathbf{0} & \mathbf{I} \end{bmatrix} \right\| = 0, \tag{13}$$

where generally ω and β are complex.

The dispersion relation above relies on the evaluation of an infinite determinant. In practice however, a finite set of harmonics only will be used. It is thus critical to determine the minimum number of harmonics necessary to accurately represent the harmonic interactions. As was previously shown for a right handed medium, whenever the modulation and medium speeds are sufficiently close (the sonic regime), higher harmonics with significant magnitudes always exist [22]. From a numerical procedure point of view, (13) may be solved for ω or β using an initial number of harmonics. (i.e, iThe number of harmonics can then be increased until the relative change in ω or β and the amplitude of the higher harmonics are below some prescribed values [23]. It is worth noting that (13) is mathematically equivalent to finding non-trivial solutions for an infinite system of homogeneous algebraic equations in infinite unknowns. A sufficient condition for an infinite determinant to converge (i.e, have a finite value) is that the sum of the off-diagonal components and the product of the diagonal elements are both absolutely convergent [37]–[39]. Infinite determinants arise in situations intimately related to the structures studied here. In fact, it first appeared in Hill's original work in lunar motion, which resulted in periodic differential equations [40], [41]. This is not surprising since an infinite set of algebraic equations emerges directly whenever the Bloch-Floquet condition is imposed. For a generic system with arbitrary unit cell configuration as well as modulation properties (such as speed and wave shape), it may be challenging to determine whenever a given determinant converges. For an indepth description of systems of infinite equations in infinite unknowns please refer to [42]–[44].

It is worth noting that due to the spatial periodicity, the $(k, k-s)$ element of any of the sub-matrices $\mathbf{X}^{(n)} = \mathbf{A}^{(n)}, \mathbf{B}^{(n)}, \mathbf{C}^{(n)}$ or $\mathbf{D}^{(n)}$ n unit cells away is related to the $(k, k-s)$ element of the above ABCD matrix as

$$X^{(n)}_{k,k-s} = e^{-is\beta_m np} X^{(0)}_{k,k-s}. \tag{14}$$

Hence, given the ABCD parameters of any unit cell, the ABCD parameters of N cells can be determined by cascading all unit cells

$$\begin{bmatrix} \mathbf{A} & \mathbf{B} \\ \mathbf{C} & \mathbf{D} \end{bmatrix}_{\text{tot}} = \prod_{k=0}^{N-1} \begin{bmatrix} \mathbf{A}^{(k)} & \mathbf{B}^{(k)} \\ \mathbf{C}^{(k)} & \mathbf{D}^{(k)} \end{bmatrix} \tag{15}$$

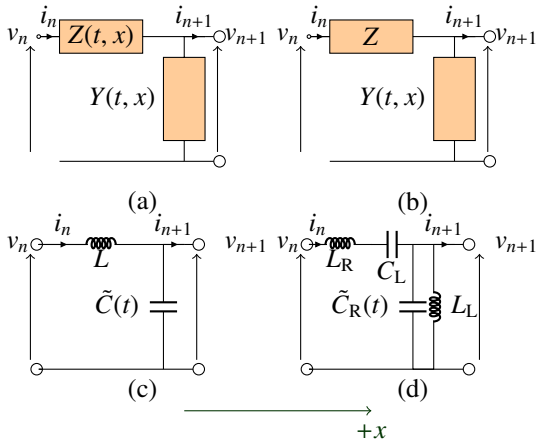

Fig. 3. One unit cell of (a) a generic time periodic TL. (b) a time periodic TL, where the periodicity is included in the shunt element. (c) a RH TL with a modulated $\tilde{C}$. (d) a modulated CRLH TL.

2) Coupled Wave Equations: Fig. 3(a) shows a circuit that consists of repeating unit cells of arbitrary series impedance and shunt admittance. Both elements can be time modulated. This structure covers many interesting TL topologies [45], [46].

In the frequency domain the circuit elements are represented by the time periodic $\mathbf{Z}$ and $\mathbf{Y}$ matrices, as was shown in subsection II-A. If the length of the unit cell p is small compared to both the operating and modulation wavelengths λ and λ_m respectively, the system can be described by per unit length quantities, where generally, $\mathbf{Z}(x) = \mathbf{Z}'(x)p$ and $\mathbf{Y}(x) = \mathbf{Y}'(x)p$. Applying KVL and KCL, and in the limit of infinitesimal p, the voltage and current can be described using the telegraphist equations

$$d\mathbf{V}/dx = -\mathbf{Z}'(x)\mathbf{I} \text{ and } d\mathbf{I}/dx = -\mathbf{Y}'(x)\mathbf{V}. \tag{16}$$

Equations (16) are general for any time periodic structures, where $\mathbf{Z}'(x)$ and $\mathbf{Y}'(x)$ can be an arbitrary functions of x. This means that (16) can be applied to spacetime periodic systems as well as to time periodic systems with an arbitrary spatial variation. By matching the boundary conditions, (16) can be used to determine the amplitudes and phases of a given wave and its time harmonics as they propagate through a cascade of different media. It is worth noting that the state variables $\mathbf{V}$ and $\mathbf{I}$ are the time harmonics at a given position x. Eqs. (16) represent an infinite system of coupled differential equations, where coupling arises from the time periodic modulation.

III. Results and Discussion

In Subsection A, we will use the time periodic circuit approach to derive the characteristic equation of a synthesized right handed transmission line (RH TL), where the length of the unit cell can be comparable to the modulation wavelength. In Subsection B we will shed some light on the dispersion relation of a general TL, where the modulation is applied to the shunt branch. Additionally, a CRLH will be closely examined.

A. RH TL Dispersion Relation

Similarly to LTI systems, a single unit cell, shown in Fig. 3 (b), can be considered as the cascade of two networks: the series LTI inductance and the shunt LTP capacitance. Hence

$$\begin{bmatrix} \mathbf{A} & \mathbf{B} \\ \mathbf{C} & \mathbf{D} \end{bmatrix} = \begin{bmatrix} \mathbf{I} & \mathbf{Z} \\ \mathbf{0} & \mathbf{I} \end{bmatrix} \begin{bmatrix} \mathbf{I} & \mathbf{0} \\ \mathbf{Y} & \mathbf{I} \end{bmatrix} = \begin{bmatrix} \mathbf{I}+\mathbf{ZY} & \mathbf{Z} \\ \mathbf{Y} & \mathbf{I} \end{bmatrix} \tag{17}$$

The matrices $\mathbf{Z}$ and $\mathbf{Y}$ are $2N+1 \times 2N+1$, where the $-N$ to N harmonics are only considered. The situation where the temporal periodicity is applied to one element only (usually the shunt capacitance) is very well understood and hence will be used as our test-case in the following discussion. In this case, the impedance matrix is diagonal,

$$Z_{kk} = i\tilde{\omega}_k L. \tag{18}$$

Time periodicity appears in the $\mathbf{Y}$ matrix, where

$$Y_{k,m} = i\tilde{\omega}_k C_{k-m}. \tag{19}$$

For monotone modulation $\tilde{C} = C_0\,(1 + M\cos(\omega t - \beta_m n p))$. Therefore, $C_{k,k} = C_0$, $C_{k,k\pm1} = MC_0/2$ and $C_{k,s} = 0$ otherwise. Substituting (18) and (19) in (17), and using (13), one arrives at the system of homogeneous equations

$$e^{i\beta_m p}V_{k+1} + e^{-i\beta_m p}V_{k-1} + \frac{2}{M}\left[1 - \left(\frac{2\sin\tilde{\beta}_k p/2}{\tilde{\omega}_k\sqrt{LC_0}}\right)^2\right]V_k = 0, \tag{20}$$

where $k = 0, \pm1, \pm2, \cdots$. The system of equations (20) is valid for an arbitrary modulation wavelength. The dispersion relation is determined from the non-trivial solution of (20). When the modulation wavelength is considerably larger than the unit cell, i.e, $\beta_m p \ll 1$ and operating in the range where the structure is homogeneous (i.e, $\tilde{\beta}_k p \ll 1$), $2\sin\tilde{\beta}_k p/2 \approx \tilde{\beta}_k p$ and (20) reduces to

$$V_{k-1} + V_{k+1} + \frac{2}{M}\left[1 - \left(\frac{\beta + k\beta_m}{\omega + k\omega_m}c\right)^2\right]V_k = 0, \tag{21}$$

where $c \equiv \lim_{p\to0} p/\sqrt{LC_0}$ is the speed of the homogeneous TL. It is convenient to normalize the wave-numbers and frequencies to be multiples of the modulation wavelength $\lambda_m \equiv 2\pi/\beta_m$. Therefore, the above equation reduces to

$$V_{k-1} + V_{k+1} + \frac{2}{M}\left[1 - \left(\frac{\beta\lambda_m + 2\pi k}{K\lambda_m + 2\pi\nu k}\right)^2\right]V_k = 0, \tag{22}$$

where $K \equiv \omega/c$, the wave number of the unmodulated TL, $\nu \equiv \nu_m/c$. Equation (22) is identical to the one derived for a modulated homogeneous medium. The circuit approach shows that such relation is only valid under the long wavelength approximations:

$$\beta_m p \ll 1,\ \tilde{\beta}_k p \ll 1. \tag{23}$$

When the above two conditions are not satisfied, one should resort to (20). This may be necessary in practical scenarios, where the TL is synthesized from *finite* unit cells. Fig. 4 shows the dispersion relations calculated using (20) and compared to (21) in the limit $M \to 0$. In this case, the dispersion relation of a general TL, determined by (20), reduces to

$$2\sin\tilde{\beta}_k p/2 = \pm p\tilde{\omega}_k/c \tag{24}$$

Additionally, the dispersion relation for a homogeneous TL is calculated from (21) as

$$\tilde{\beta}_k = \pm\tilde{\omega}_k/c \tag{25}$$

As illustrated in Fig. 4, the scattering centers are shifted down in frequency due to the bending of the dispersion curves, where $2\sin\tilde{\beta}_k p/2$ deviates from $\tilde{\beta}_k p$. Bending is associated with the reduction of the group velocity, which is equal to the energy flow velocity [47]. In turn, the energy flow velocity is directly proportional to the Bloch impedance. As frequency increases, the Bloch impedance decreases (can be attributed to an increase in the equivalent capacitance of the TL), resulting in a reduction in energy flow. The bending of the dispersion curves is particularly observed when $\beta_m p$ becomes large and is exhibited more in higher harmonics $\tilde{\beta}_k = \beta + k\beta_m,\ k \geq 1$. The scattering frequencies represent the intersection of two curves given by the above equation. For instance, the first Anti-Stokes' (backward) center [18] is determined from the intersection of the negative branch of the 0^{th} curve with the positive branch of the $+1$ curve, which are given by

$$\sin(\beta + 2\pi)\,p/2 + \sin\beta p/2 = \pi\nu p,\ \text{ and } Kp = -2\sin\beta p/2. \tag{26}$$

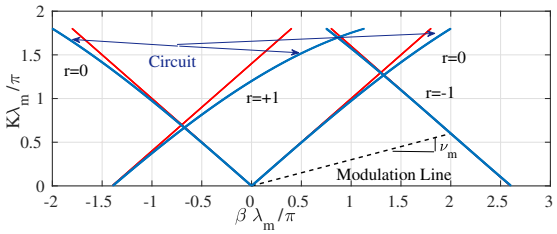

Fig. 4. Dispersion Relation for $\nu = 0.3$, $M \to 0$, using the time periodic circuit and long wavelength (homogeneous) approximation.

To examine the behaviour for macroscopic unit cells, the dispersion relations (20) and (21) are solved for different λ_m

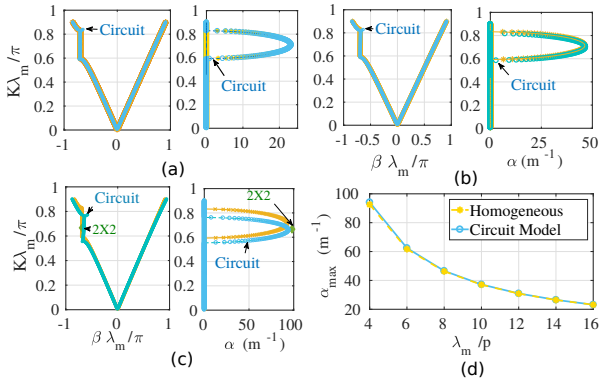

Fig. 5. Dispersion Relation for $\nu = 0.3$, $M = 0.5$, using the time periodic circuit and long wavelength (homogeneous) approximation. (a)$\lambda_m/p = 16$, (b) $\lambda_m/p = 8$, (c) $\lambda_m/p = 4$, (d) maximum α.

values when $\nu = 0.3$ and $M = 0.5$. The results are reported in Fig. 5, where the Anti-Stokes' center is only considered. Inside the bandgap, the incident wave number become complex: $\beta - i\alpha$, where α is the attenuation constant. As λ_m decreases the scattering center is shifted to a lower frequency value, as expected from the bending of the dispersion curves (Fig. 4). Since the scattering center is the intersection of the 0^{th} and 1^{st} harmonics, the system of equations (20) can be reduced to the 2×2 secular equation

$$\begin{vmatrix} D_0 & e^{i\beta_m p} \\ e^{-i\beta_m p} & D_{+1} \end{vmatrix} = 0, \text{ or } D_0 D_{+1} = 1. \tag{27}$$

The position and strength of the Anti-Stokes' center are calculated using (26) and (27) as shown in Fig. 5 (c). The 2×2 system accurately predicts the frequency of the scattering center. However, it *slightly* over estimates the value of the attenuation constant. It is worth noting that, *formally*, (27) has been employed to study wave propagation and radiation from modulated surfaces [48], [49].

Additionally, Fig. 5 (d) shows that even when λ_m becomes just a few unit cells long, α is still inversely proportional to λ_m. This implies that, given a fixed modulation speed v_m, the insertion loss is directly proportional to the modulation frequency and such a relation is valid even when λ_m is just few times larger than p. It is worth noting too that the behaviour for macroscopic unit cells solely depends on the bend of the dispersion curves. The coefficients $\exp(-i\beta_m p)$ and $\exp(i\beta_m p)$ appearing in the off-diagonal terms in the 2×2 determinant (27) have no influence. They only affect the phase difference between the 0^{th} and $+1^{\text{st}}$ harmonics.

To verify the behaviour for small λ_m values, a time domain analysis of the transmission line is performed using a state space model (SSM) [50]. In this case, a finite number of unit cells is used, KCL and KVL along with the circuital relations are applied in the time domain, resulting in the system of ordinary differential equations (ODEs) (1). The ODEs are solved using Runge-Kutta method, hence SSM enables the solution of arbitrary circuits in the time domain (regarded in this aspect as a transient solver) [32]. From the computed time domain voltages, the magnitude and phase of the time

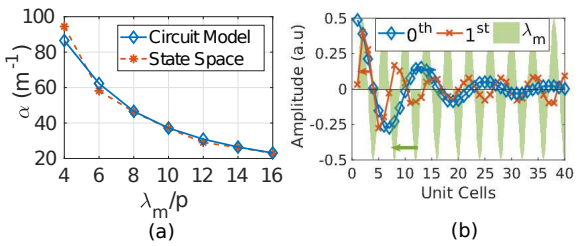

Fig. 6. (a) Attenuation constant α calculated at the normalized frequency $Ka = \pi(1-\nu)$ using the dispersion relation and state space model. (b) Amplitude of incident and scattered signals near the Anti-Stoke's scattering center calculated using SSM. The arrows indicate the direction of propagation of the modulation and the +1 harmonic.

harmonics at each node are calculated using a fast Fourier transform. Fig. 6 (a) shows α calculated using SSM and secular equation (13) at the Anti-Stokes' center ($Ka = \pi(1-\nu)$) for different values of λ_m/p. As λ_m/p decreases, α increases. Fig. 6 (b) shows the amplitude of the incident and scattered waves superimposed on the modulation wave. The modulating wavelength is four unit cells. The incident wave attenuates as it propagates through the structure due to the scattering in the +1 mode that bounces back toward the source. Furthermore when $\lambda_m/p = 4$, the normalized frequency at which the maximum attenuation occurs is shifted from 0.7π to 0.66π due to the bend of the dispersion curves (Fig. 4). At this frequency the SSM predicts $\alpha_{\max}$ to be 99.57 m^{-1}, very close to the value predicted by the 2×2 secular equation ($\alpha_{\max} = 98.12$ m^{-1}).

1) Time periodic S parameters: Instead of the dispersion relation, the circuit model presents another complementary view of the interaction process that may lead to non-reciprocity. Given the number of stages, the total ABCD matrix can be calculated using (15), from which the scattering parameters are obtained. It is worth noting that the spatial modulation is only used to modify the appropriate terms in the ABCD matrices as given by (14). The time periodic S parameters are shown in Fig. 7. Noting that $S_{21}^{(0,0)}$ ($S_{12}^{(0,0)}$) represents the scattering in the forward (backward) direction, it is clear that the isolation occurs in the bandgaps, where the transmission coefficients are significantly reduced. The $S_{11}^{(r,0)}$ parameters show that, inside the forward bandgap, scattering occurs at the -1 harmonic as expected (1^{st} Stokes' centers) [18], [23]. Additionally, scattering in the +1 harmonic occurs for the backward interaction (1^{st} Anti-Stokes' center). Moreover, there is another interaction at the 2^{nd} backward scattering center due to the coupling between the fundamental signal and its second harmonic.

Similarly to LTI systems, the scattering parameters can be used to estimate the dispersion relation. Ignoring the inhomogenity in the Bloch impedance due to the finite length of the TL and scattering in time harmonics, the forward (backward) transmission coefficient $S_{21}^{(0,0)}$ ($S_{12}^{(0,0)}$) assumes the form $S_{21}^{(0,0)} = \exp\left([-\alpha^F - i\beta^F]L\right)$ ($S_{12}^{(0,0)} = \exp\left([-\alpha^B - i\beta^B]L\right)$, where L is the TL total length. Therefore knowing $S_{21}^{(0,0)}$ ($S_{12}^{(0,0)}$), enables the estimation of α^F and β^F (α^B and β^B).

Fig. 8 shows the estimated α and β for 100 unit cells. Qualitatively, the S parameters can be used to estimate the

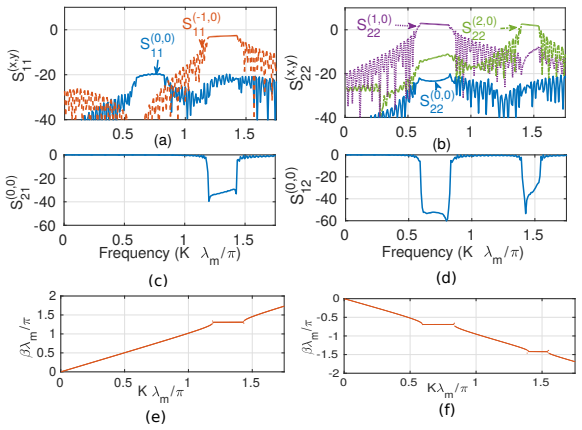

Fig. 7. Generalized S parameters for $\nu = 0.3$, $M = 0.5$, using the time periodic circuit when $\lambda_m/p = 8$. Forward direction: (a) scattering. (c) transmission. (e) dispersion. Backward: (b) scattering. (d) transmission. (f) dispersion.

position and width of the bandgaps. It is, however, not as accurate as the dispersion relations (13). This is mainly due to the inhomogenity of the Bloch impedance inside the bandgap resulting from the increased scattering in time harmonics. Additionally, the finite number of unit cells used to calculate the S parameters inevitably adds to the inaccuracy of the estimation.

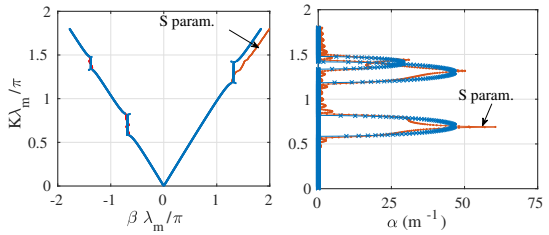

Fig. 8. (Left) Dispersion Relation calcuated using the secular equation (13) and the time periodic S parameters. (Right) Attenation constant calculated (13 and S parameters.

2) Coupled Wave Equations of spacetime periodic RH TL: The time periodic telegraphist's equations (16) are readily applicable to the RH TL, where the shunt capacitance is space-time modulated. The telegraphist equations can be combined to produce the second order matrix equation

$$d^2\mathbf{V}/dx^2 = \mathbf{Z}'\mathbf{Y}'(x)\mathbf{V}, \tag{28}$$

which represents the interaction of an infinite number of waves. To illustrate the usefulness of the coupled wave representation (28), the interaction of the fundamental with its +1 harmonic is analyzed. Such interaction is significant at the Anti-Stokes' scattering center [18], [23].

For monotone modulation, using (18) and (19),

$$d^2V_0/dx^2 = -(\omega/c)^2 V_0 - (\omega/c)^2 (M/2) e^{i\beta_m x} V_1 \tag{29}$$

and

$$\frac{d^2V_1}{dx^2} = -\left(\frac{\omega+\omega_m}{c}\right)^2 \frac{M}{2} e^{-i\beta_m x} V_0 - \left(\frac{\omega+\omega_m}{c}\right)^2 V_1 \tag{30}$$

If $V_0 = A_0 \exp(-i\beta x)$ it follows that $V_1 = A_1 \exp(-i[\beta+\beta_m]x)$; implying that the harmonics satisfy the phase matching condition. Substituting these expressions back in (29) and (30) results in a secular equation in ω and β

$$\left(\frac{2}{M}\right)^2 \left[1 - \left(\frac{\beta\lambda_m}{K\lambda_m}\right)^2\right]\left[1 - \left(\frac{\beta\lambda_m + 2\pi}{K\lambda_m + 2\pi\nu}\right)^2\right] - 1 = 0, \tag{31}$$

identical to (27) under the long wavelength approximation.

B. General Ladder TL

In this subsection, we demonstrate how the dispersion relation (13) can be applied to a generic TL that is formed of unit cells consisting of series and shunt impedances as shown in Fig. 3(b). Such a structure covers the RH TL studies in the previous subsections and the composite right left handed (CRLH) TL presented in Fig. 3(d). The time periodicity is assumed to be purely sinusoidal and added to the shunt admittance only. Such a restriction simplifies the mathematical treatement and allows one to focus on the propagation properties of systems with the generic unit cells depicted in Fig. 3(b). The sinusoidal modulation permits the reduction of the dispersion relation to the three term recursion relation [51], [52]

$$A_k V_{k+1} + B_k V_k + C_k V_{k-1} = 0, \tag{32}$$

where the coefficients $A_k \equiv Z_{k,k}Y_{k,k+1}\exp(i\beta_m p)$, $B_k \equiv Z_{k,k}Y_{k,k} + 4\sin^2\tilde{\beta}_k p/2$ and $C_k \equiv Z_{k,k}Y_{k,k-1}\exp(-i\beta_m p)$, and the phase of the modulation is taken such that $Y_{k,k-1} = Y_{k,k+1}$. Eq. (32) is the generalized form of (20). Unlike (22), first appeared in [22], [23] for a RH media, (32) is applicable to arbitrary unit cells and to situations where the unit cell length cannot be ignored. If modulation is not purely sinusoidal then (32) becomes a $2N+1$ recursion, where N is the number of significant modulation harmonics. It may be challenging, however, to find an analytical closed form expression for an arbitrary $2N+1$ recursion relation. Fortunately, the three term recursive relation (32) can be reduced to the canonical form $y_{k+1} + y_{k-1} - D_k y_k = 0$, by the change of variables: $\alpha_0 = \alpha_1 = 1$, $\alpha_{k+1}A_k = \alpha_{k-1}C_k, \forall k \geqslant 1$, $V_k = \alpha_k y_k$ and $D_k = -(\alpha_k/\alpha_{k+1})(B_k/A_k)$ [51]. Therefore, when

$$\alpha_{2n} = \alpha_{2n+1} = e^{-i2n\beta_m p}, \; n = 0, \pm, 1, \cdots, \tag{33}$$

(32) reduces to the canonical form, where

$$D_k = -\frac{Z_{k,k}Y_{k,k} + 4\sin^2\tilde{\beta}_k p/2}{Z_{k,k}Y_{k,k+1}} e^{-i\beta_m p(-1)^k}. \tag{34}$$

A sufficient condition that guarantees the convergence of the space-time harmonics expansion is the existence of some N such that for all $n > N$, $|D_n| > 2$ [48] . As was previously shown, for the three term recursion, the infinite determinant (13) can be reduced to a continued fraction expansion.

As a typical example, consider the CRLH TL shown in Fig. 3(d). Here the time periodicity is introduced via the modulation of the shunt capacitance C_R. The balanced configuration where the shunt and series resonances are equal ($\omega_{se} = 1/\sqrt{L_R C_L} = \omega_{sh} = 1/\sqrt{L_L C_R}$) is assumed to hold in

the absence of the time periodicity. Since C_R mainly impacts the right hand regime, $Y_{k,k-1}$ is taken to be $0.8Y_{k,k}$; hence making the interaction of space-time harmonics in the left hand regime observable. Additionally, the circuit components (C_R, C_L, L_R, L_L) are chosen such that $\omega_{se} = \omega_{sh} = 1$ a.u. The modulation frequency is set to 1.2 (a.u), just above ω_{se} and $\beta_m p = 0.7$. These values guarantee that the main branch ($r = 0$) and the $r = \pm 1$ branches intersect in both the left and right hand regimes (Fig. 9(a)). The continued fraction expansion approach is used to calculate β for any given frequency ω. The continued fraction is calculated using Euler-Wallis recursive relation [53]. Twenty five harmonics are included to assure the convergence of the continued fraction expansion. However a much lower number of harmonics is sufficient, since the continued fraction rapidly converges.

Figs. 9(a) and (b) depict the calculated real and imaginary parts of β, respectively. The forward (backward) direction is defined to be $\beta_m \mathrm{Re}(\beta) > 0$ ($\beta_m \mathrm{Re}(\beta) < 0$). In Figs. 9(a) and (c), β_m is taken to be positive, therefore the forward (backward) direction is equivalent to $\mathrm{Re}(\beta) > 0$ ($\mathrm{Re}(\beta) < 0$). As shown, there are two main interactions in both the forward and backward directions that result in bandgaps: (1) the *usual* RH-RH bandgap, appearing between $\omega = 1.2 - 1.7$, which behaves very similar to the bandgap of a modulated RH TL. It is formed due to the interaction in the RH regimes of the $r = 0$ and $r = -1$ branches. (2) The LH-LH bandgap (of a smaller magnitude appearing around $\omega = 0.7$), however, is due to the interaction of the left handed wave with its $r = \pm 1$ harmonic. To reproduce the dispersion relations, a 40 unit cells CRLH TL is directly simulated in the time domain. The real and imaginary parts of the wave number are estimated from the spectrum of the time domain data. The results are presented in Fig. 9(c) and (d).

Inside the FWD bandgaps $\mathrm{Re}(\beta) > 0$. This means that, unlike the RH-RH interaction, the group velocity and modulation directions are contra-directed inside the LH-LH bandgap (due to the left-handensess of the medium, group and phase velocities have opposite directions). Therefore to observe nonreciprocity, the excitation is applied to one side of the medium for a RH-RH bandgap and to the other for the LH-LH bandgap. Similar arguments apply to the backward situation.

C. General Space Time periodic Modulation

In this subsection we consider (28) for a general topology and arbitrary space modulation. The k^{th} time harmonic obeys

$$dV_k^2/dx^2 = \sum_{r=-\infty}^{\infty} Z_{kk}(\omega) Y_{kr}(x,\omega) V_r, \tag{35}$$

where $Z_{kk}(\omega) = Z_{00}(\tilde{\omega}_k)$, $Y_{k,r}(x,\omega) = Y_{0,r-k}(x,\tilde{\omega}_k)$. $Y_{k,r}$ is in general a function of x. Of a particular importance is the subclass of travelling wave modulations $y(x,t) = y(x - v_m t)$. In this case, $Y_{k,r}(x,\omega) = \hat{Y}_{k,r}(\omega)\exp(-i[k-r]\beta_m x)$. Therefore seeking a solution $V_k = A_k \exp(-i\tilde{\beta}_k x)$, converts (28) into a system of algebraic equations,

$$\sum_{r=-\infty, r\neq k}^{\infty} Z_{00}(\tilde{\omega}_k)\hat{Y}_{0,r-k}(\tilde{\omega}_k)A_r + \left(Z_{00}(\tilde{\omega}_k)\hat{Y}_{0,0}(\tilde{\omega}_k) + \tilde{\beta}_k^2\right)A_k = 0, \tag{36}$$

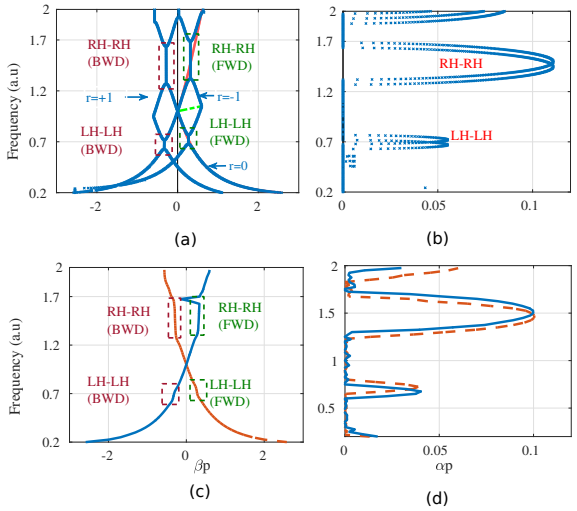

Fig. 9. (a), (b) Real and imaginary of the wave number of a CRLH TL calculated using (32). The RH (LH) regime is where both the phase and group velocities are co-directional (contra-directional). (c), (d) Real and imaginary of the wave number using SSM.

or compactly as the matrix equation

$$\mathcal{S}\mathbf{A} = 0. \tag{37}$$

The above infinite set of equations can be truncated to a finite set such that r runs from $-N$ to N. A non-trivial solution can be found by forcing the determinant of $\mathcal{S}$ to be zero. The determinant $\Delta(\omega,\beta)$ is a function of the complex frequency ω and/or complex wave propagation β. The harmonics $A_{-N}, \cdots, A_N$ form a $2N+1$ complex vector space. Hence, the solution vector $\mathbf{A} \in$ null $\mathcal{S}$, or equivalently it is the eigenvector of $\mathcal{S}$ that corresponds to a zero eigenvalue.

Given the input frequency ω an optimization procedure can be applied to compute β that minimizes some norm of $\Delta(\omega,\beta)$. However, it is crucial to point out here that the value of Δ scales with the number of harmonics N. To apply a norm that does not depend on N, we exploit the fact that Δ is the product of all eigenvalues of $\mathcal{S}$. Therefore, the minimization criterion is reduced to finding β that guarantees $\min(|\mathrm{eigvalue}(\mathcal{S})|) < \delta$, where δ is a small number taken here to be 10^{-9}. To demonstrate how the above procedure

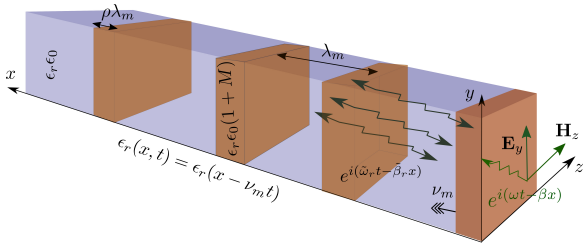

Fig. 10. Space-time modulated RH media. The relative permittivity ϵ_r is modulated by a travelling rectangular wave with a duty cycle ρ. The wiggly arrows inside the media depicts the spacetime harmonics $\exp i(\tilde{\omega}_r t - \tilde{\beta}_r x)$.

can be applied to a particular scenario, consider the RH media shown in Fig. 10. The relative permittivity of a RH medium is modulated by a rectangular travelling wave, where ϵ_r changes from ϵ_r to $\epsilon_r(1+M)$. The duty cycle ρ controls the

strength of the higher harmonics. While keeping ρM fixed, as ρ decreases, the amplitudes of the higher harmonics relative to the fundamental increase [54]. The Fourier coefficients are

$$\tilde{\epsilon}_{rq} = \begin{cases} \epsilon_r(1+\rho M) & q=0 \\ i\frac{M\epsilon_r}{2\pi q}\left(e^{-i2\pi\rho q}-1\right) & \text{otherwise.} \end{cases} \tag{38}$$

Noting the analogy between a RH media and a RH TL, (36) can be written as

$$\sum_{q\neq k}^{\infty} \frac{iM}{1+\rho M}\frac{1-e^{i2\pi\rho q}}{2\pi q}A_q + \left[1-\frac{1}{1+\rho M}\left(\frac{\beta\lambda_m+2\pi k}{K\lambda_m+2\pi\nu k}\right)^2\right]A_k = 0. \tag{39}$$

For sufficiently small ρ (i.e, $\rho q \ll 1$), the coefficient of A_q becomes independent of the mode number q.

Figure 11 presents the simulation results when $\rho = 0.1$ and for two different values of M and N. For the lowest order bandgaps, both in the forward and backward direction, the $N = 16$ calculation provided slightly higher values of α due to the coupling with higher harmonics. The calculated values were in a very good agreement with Finite Difference Time Domain (FDTD) simulations. More interestingly is the behaviour near the second order bandgap, arising from the interaction of the main branch ($q = 0$) with the second order branch ($q = +2$). It is clear that a purely sinusoidal approximation of the modulation (using $N = 1$) underestimates both the gap strength and width. This is mainly due to the neglection of the second harmonic that considerably interacts with the main branch; particularly for small ρ values, where the modulation higher harmonics cannot be ignored. Although $N = 16$ was used to compute the dispersion relation in Fig. 11, it is sufficient to use $N = 2$ inside the second order bandgap since the interaction is mainly with the second harmonic. Fig. 12(a) presents the amplitude of the fields of the fundamental harmonic and its two higher harmonics ($\omega+\omega_m$ and $\omega+2\omega_m$) calculated inside the modulated media using FDTD. Although the fundamental harmonic interacts with its $\omega+\omega_m$ harmonic, its main interaction is with the second harmonic, agreeing with the dispersion relation in Fig. 11. Amplitude reductions of more than 40 dB cannot be directly computed from the FDTD simulated data due to limited dynamic range of the FDTD method [55]. Therefore, α is calculated by fitting the peaks of the amplitudes to an exponential function. Additionally, the computed spectrum of the scattered field and the eigenvector when the frequency is in the middle of the second bandgap (Fig. 12(b) and (c), respectively) further strengthen this implication. It is worth noting that inside the second order bandgap the dispersion relation can be approximated by a 3×3 system of linear homogeneous equations in A_0, A_1, A_2. The main interaction between the fundamental and second harmonic results in an active in-elastic scattering. Nevertheless, there is a non-vanishing interaction with the first harmonic, as Figs. 12(a) and (b) show and verified by the calculated eigenvector presented in Fig. 12(c). After approx. $5\lambda_m$, the fundamental and second harmonics magnitudes are significantly decayed, leaving the effect of the first harmonic dominant in the far end. It was shown in [23] that for sinusoidal modulation the attenuation inside the bandgaps decreases as the order of the bandgap increases; therefore limiting parametric conversion to the +1 harmonic only. As demonstrated here however, nonsinusoidal modulation enables the strong interaction with higher order harmonics, which potentially can be harnessed to provide strong parametric conversions to higher harmonics.

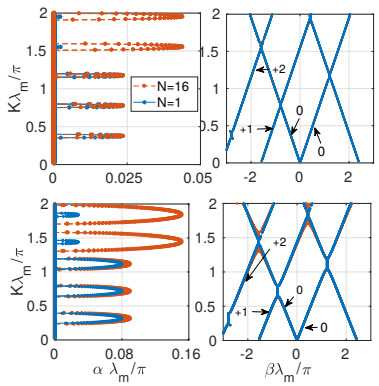

Fig. 11. Dispersion Relation for a rectangular travelling wave modulation of a RH medium. (Top): $M = 0.5$, $\rho = 0.1$. (Bottom): $M = 2$, $\rho = 0.1$.

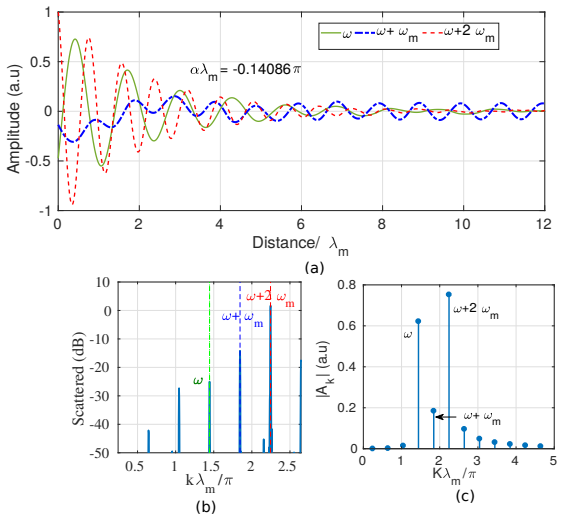

Fig. 12. (a) Amplitude of the input signal and its first two harmonics at $\omega+\omega_m$ and $\omega+2\omega_m$; all inside the modulated medium ($M = 2$ and $\rho = 0.1$). The input signal is a plane wave with a frequency ω that impinges the medium at normal incidence. (b) Spectrum of the scattered signal. (c) Eigenvector when the input frequency ω is in the middle of the second bandgap ($K\lambda_m = 1.44\pi$).

IV. Conclusion

A circuit formalism for time periodic circuits is used to determine the dispersion relation of an arbitrary space-time periodic stucture. The relation is valid even when the length of the spatial periodicity is comparable to the modulating and operating wavelengths. In this case, the scattering centers are shifted to lower frequencies due to the bending of the dispersion relation. For infinitesimal unit cells, the relation retains the formula that was perviously derived for homogeneous media. Additionally, the system can be described by a generalized telegraphist's equations. Generally, the time harmonics are coupled by the time periodic circuit elements. The circuit based approach permits the use of S parameters to describe scattering and modal conversion in different time harmonics.

References

[1] D. L. Sounas, C. Caloz, and A. Alù, "Giant non-reciprocity at the subwavelength scale using angular momentum-biased metamaterials," *Nature Communications*, vol. 4, p. 2407, 2013.

[2] N. A. Estep, D. L. Sounas, and A. Alù, "Magnetless microwave circulators based on spatiotemporally modulated rings of coupled resonators," *IEEE Transactions on Microwave Theory and Techniques*, vol. 64, no. 2, pp. 502–518, 2016.

[3] A. Kord, D. L. Sounas, and A. Alù, "Magnet-less circulators based on spatiotemporal modulation of bandstop filters in a Delta topology," *IEEE Transactions on Microwave Theory and Techniques*, vol. 66, no. 2, pp. 911–926, Feb 2018.

[4] Y. Hadad, J. C. Soric, and A. Alù, "Breaking temporal symmetries for emission and absorption," *Proceedings of the National Academy of Sciences*, vol. 113, no. 13, pp. 3471–3475, 2016.

[5] S. Taravati and C. Caloz, "Mixer-duplexer-antenna leaky-wave system based on periodic space-time modulation," *IEEE Transactions on Antennas and Propagation*, vol. 65, no. 2, pp. 442–452, 2017.

[6] D. Ramaccia, D. L. Sounas, A. Alù, F. Bilotti, and A. Toscano, "Nonreciprocity in antenna radiation induced by space-time varying metamaterial cloaks," *IEEE Antennas and Wireless Propagation Letters*, vol. 17, no. 11, pp. 1968–1972, Nov 2018.

[7] S. Taravati and A. A. Kishk, "Dynamic modulation yields one-way beam splitting," *arXiv preprint arXiv:1809.00347*, 2018.

[8] H. Lira, Z. Yu, S. Fan, and M. Lipson, "Electrically driven nonreciprocity induced by interband photonic transition on a silicon chip," *Phys. Rev. Lett.*, vol. 109, p. 033901, Jul 2012.

[9] J. N. Winn, S. Fan, J. D. Joannopoulos, and E. P. Ippen, "Interband transitions in photonic crystals," *Phys. Rev. B*, vol. 59, pp. 1551–1554, Jan 1999.

[10] Y. Hadad, D. L. Sounas, and A. Alù, "Space-time gradient metasurfaces," *Phys. Rev. B*, vol. 92, p. 100304, Sep 2015.

[11] Y. Mazor and A. Alù, "One-way hyperbolic metasurfaces based on synthetic motion," *arXiv preprint arXiv:1902.02653*, 2019.

[12] M. Mirmoosa, G. Ptitcyn, V. Asadchy, and S. Tretyakov, "Time-varying reactive elements for extreme accumulation of electromagnetic energy," *Phys. Rev. Applied*, vol. 11, p. 014024, Jan 2019.

[13] A. Shlivinski and Y. Hadad, "Beyond the bode-fano bound: Wideband impedance matching for short pulses using temporal switching of transmission-line parameters," *Physical review letters*, vol. 121, no. 20, p. 204301, 2018.

[14] R. M. Fano, "Theoretical limitations on the broadband matching of arbitrary impedances," *Journal of the Franklin Institute*, vol. 249, no. 1, pp. 57–83, 1950.

[15] S. Taravati, "Giant linear nonreciprocity, zero reflection, and zero band gap in equilibrated space-time-varying media," *Physical Review Applied*, vol. 9, no. 6, p. 064012, 2018.

[16] S. Taravati and A. A. Kishk, "Space-time modulation: Principles and applications," *arXiv preprint arXiv:1903.01272*, 2019.

[17] G. Trainiti and M. Ruzzene, "Non-reciprocal elastic wave propagation in spatiotemporal periodic structures," *New Journal of Physics*, vol. 18, no. 8, p. 083047, 2016.

[18] S. Y. Elnaggar and G. N. Milford, "Controlling non-reciprocity using enhanced brillouin scattering," *IEEE Transactions on Antennas and Propagation*, 2018.

[19] P. Tien, "Parametric amplification and frequency mixing in propagating circuits," *Journal of Applied Physics*, vol. 29, no. 9, pp. 1347–1357, 1958.

[20] A. Cullen, "A travelling-wave parametric amplifier," *Nature*, vol. 181, no. 4605, pp. 332–332, 1958.

[21] J.-C. Simon, "Action of a progressive disturbance on a guided electromagnetic wave," *IRE Transactions on Microwave Theory and Techniques*, vol. 8, no. 1, pp. 18–29, 1960.

[22] A. A. Oliner and A. Hessel, "Wave propagation in a medium with a progressive sinusoidal disturbance," *IRE Transactions on Microwave Theory and Techniques*, vol. 9, no. 4, pp. 337–343, July 1961.

[23] E. S. Cassedy and A. A. Oliner, "Dispersion relations in time-space periodic media: Part i; stable interactions," *Proceedings of the IEEE*, vol. 51, no. 10, pp. 1342–1359, Oct 1963.

[24] E. S. Cassedy, "Dispersion relations in time-space periodic media part ii; unstable interactions," *Proceedings of the IEEE*, vol. 55, no. 7, pp. 1154–1168, July 1967.

[25] S. Qin, Q. Xu, and Y. E. Wang, "Nonreciprocal components with distributedly modulated capacitors," *IEEE Transactions on Microwave Theory and Techniques*, vol. 62, no. 10, pp. 2260–2272, 2014.

[26] C. Kurth, "Steady-state analysis of sinusoidal time-variant networks applied to equivalent circuits for transmission networks," *IEEE Transactions on Circuits and Systems*, vol. 24, no. 11, pp. 610–624, 1977.

[27] N. M. Wereley and S. R. Hall, "Linear time periodic systems: Transfer function, poles, transmission zeroes and directional properties," in *1991 American Control Conference*, June 1991, pp. 1179–1184.

[28] R. Trinchero, I. S. Stievano, and F. G. Canavero, "Steady-state response of periodically switched linear circuits via augmented time-invariant nodal analysis," *Journal of Electrical and Computer Engineering*, vol. 2014, p. 25, 2014.

[29] R. Telichevesky, K. Kundert, and J. White, "Receiver characterization using periodic small-signal analysis," in *Proceedings of Custom Integrated Circuits Conference*. IEEE, 1996, pp. 449–452.

[30] R. E. Collin, *Foundations for microwave engineering*. John Wiley & Sons, 2007.

[31] N. A. Estep, D. L. Sounas, J. Soric, and A. Alù, "Magnetic-free non-reciprocity and isolation based on parametrically modulated coupled-resonator loops," *Nature Physics*, vol. 10, no. 12, p. 923, 2014.

[32] O. Wing, *Classical circuit theory*. Springer Science & Business Media, 2008, vol. 773.

[33] S. Y. Elnaggar and G. N. Milford, "Description and stability analysis of nonlinear transmission line type metamaterials using nonlinear dynamics theory," *Journal of Applied Physics*, vol. 121, no. 12, p. 124902, 2017.

[34] R. K. Miller and A. N. Michel, *Ordinary Differential Equations*. Academic Press, 1982.

[35] D. M. Pozar, *Microwave Engineering 3e*. Wiley, 2006.

[36] S. Elnaggar and G. Milford, "Three wave mixing as the limit of nonlinear dynamics theory for nonlinear transmission line type metamaterials," *IEEE Transactions on Antennas and Propagation*, vol. 66, no. 1, 2018.

[37] E. T. Whittaker and G. N. Watson, *A course of modern analysis*, 4th ed. Cambridge university press, 1996.

[38] R. Mennicken, "On the convergence of infinite Hill-type determinants," *Archive for Rational Mechanics and Analysis*, vol. 30, no. 1, pp. 12–37, 1968.

[39] E. H. Roberts, "Note on infinite determinants," *The Annals of Mathematics*, vol. 10, no. 1/6, pp. 35–49, 1895.

[40] W. Magnus *et al.*, "Infinite determinants associated with Hill's equation," *Pacific Journal of Mathematics*, vol. 5, no. Suppl., pp. 941–951, 1955.

[41] C. Curtis and B. Deconinck, "On the convergence of Hills method," *Mathematics of computation*, vol. 79, no. 269, pp. 169–187, 2010.

[42] F. Riesz, *Les systèmes d'équations linéaires à une infinité d'inconnues (French)*. Paris, 1913, vol. 19.

[43] F. M. Fedorov, "Introduction to the theory of infinite systems. theory and practices," *AIP Conference Proceedings*, vol. 1907, no. 1, p. 020002, 2017.

[44] F. Fedorov, N. Pavlov, O. Ivanova, and S. Potapova, "Quasihomogeneous infinite systems of linear algebraic equations," in *Journal of Physics: Conference Series*, vol. 1141, no. 1. IOP Publishing, 2018.

[45] C. Caloz and T. Itoh, *Electromagnetic metamaterials: transmission line theory and microwave applications*. John Wiley & Sons, 2005.

[46] G. V. Eleftheriades and K. G. Balmain, *Negative-refraction metamaterials: fundamental principles and applications*. John Wiley & Sons, 2005.

[47] A. Bers, "Note on group velocity and energy propagation," *American Journal of Physics*, vol. 68, no. 5, pp. 482–484, 2000.

[48] A. Oliner and A. Hessel, "Guided waves on sinusoidally-modulated reactance surfaces," *IRE Transactions on Antennas and Propagation*, vol. 7, no. 5, pp. 201–208, 1959.

[49] R. Collin and Z. FJ, *"Antenna theory, Part 2'*, 1969, vol. 7.

[50] S. Y. Elnaggar and G. N. Milford, "Description and stability analysis of nonlinear transmission line type metamaterials using nonlinear dynamics theory," *Journal of Applied Physics*, vol. 121, no. 12, p. 124902, 2017.

[51] J. Meixner and F. W. Schäfke, *Mathieusche Funktionen und Sphäroidfunktionen: mit Anwendungen auf physikalische und technische Probleme (German)*. Springer-Verlag, 2013, vol. 71.

[52] L. Lorentzen and H. Waadeland, *Continued fractions with applications, volume 3 of Studies in Computational Mathematics*. North-Holland, 1992.

[53] R. M. Dudley. (2014) Continued fractions, lecture notes, math lecture series, massachusetts institute of technology. [Online]. Available: https://math.mit.edu/ rmd/IAP/continuedfractions.pdf

[54] S. Haykin, *Communication systems*. John Wiley & Sons, 2008.

[55] A. Taflove and S. C. Hagness, *Computational electrodynamics*. Artech house publishers, 2000.